THE OPTICAL PROPERTIES OF CIRCUMSTELLAR AND INTERSTELLAR DUST IN THE MID-IR

B. PEGOURIE and R. PAPOULAR
CEN-Saclay, Service d'Astrophysique
91191 Gif-sur-Yvette, Cédex, France

ABSTRACT. We deduce the optical efficiency $Q(\lambda)/a$ of the circumstellar dust material over the range 8-30 μm from twelve M and G giants and supergiants and that of the dust present in the general ISM and molecular clouds from thirteen protostars. We then discuss the differences between these two profiles in the light of the condensation theory.

1. INTRODUCTION

The IR spectrum of oxygen-rich stars is characterized by two important bands at 10 and 20 μm ascribed to silicates (Woolf and Ney, 1969). These features are visible in absorption in HII regions, molecular clouds and protostars spectra, and in the general interstellar extinction curve. The absorption profile is then narrow and peaks at 9.5 μm. One finds them in emission in young stars, M giants and supergiants, novae and supernovae. In these cases, the emission features are generally wider (FWHH from 2.5 to 3.6 μm) and their wavelength of maximum intensity is around 10 μm.

Up to now, neither meteoritic nor laboratory materials permit to precisely reproduce the emission observations. That is why we adopted the inverse attitude: the empirical determination of the optical properties of dust between 8 and 30 μm, from objects with a simple structure to permit without ambiguity the Q/a profiles extraction.

In Sect.2, we present quickly the choice criteria for the sources and the method we used. We then present in Sect.3 two profiles deduced from emission and absorption observations and show in Sect.4 how condensation and thermodynamic computations permit to understand the observed differences.

2. DESCRIPTION OF THE METHOD

2.1. Each object consists of a central star surrounded by a spherical dust shell. The envelope contribution to the total flux between 8 and 30 μm (i.e. the IR excess) is obtained by subtracting from the total flux the stellar continuum extrapolated from the photometric HKLM points.

R. H. Giese and P. Lamy (eds.), Properties and Interactions of Interplanetary Dust, 267–271.

The large variety of emission profiles (fig.2) can be understood if large grain radii are allowed (Papoular and Pégourié, 1983). Figure 1 shows the silicates ' optical efficiency between 8 and 13 μm for different grain sizes as predicted by theoretical computations which also predict that, for a grain radius $\lesssim 0.3$ μm, the optical properties in that range of wavelength become independent of a. The variation of the shape of the band with a is clearly similar to that of the IR excess of the three stars shown in fig.2.

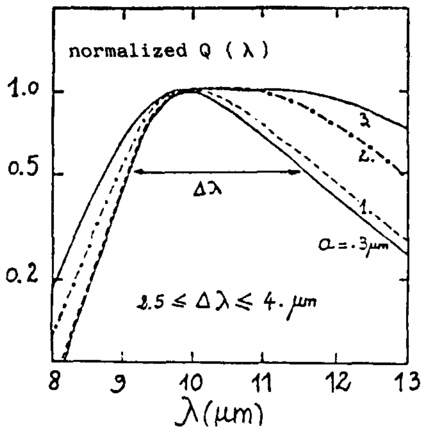

Fig.1. : Mie computations of silicates' optical efficiency for a grain radius varying from 0.3 to 3 μm.

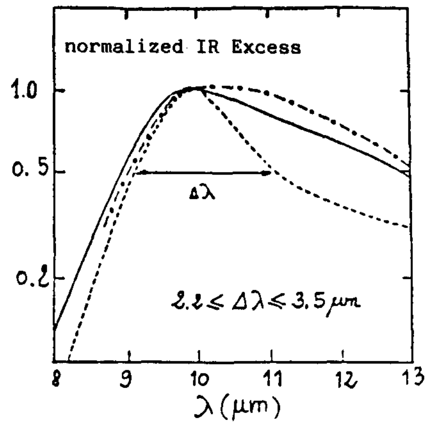

Fig.2: IR excess between 8 and 13 μm for ----TZ Cas, ——— R Leo, and —-- RCnc.

Many M supergiants exhibit a strong and narrow excess (identical to that of TZ Cas) indicating small grains and small optical depth, i.e. the best conditions to have a strong similarity between the IR excess and the dust's optical properties profile.

2.2. Similarly, favorable conditions for the analysis of absorption features will be found in the case of young objects like protostars embedded in dense molecular clouds which are expected to reflect the properties of dust in the local ISM, at least in composition.

2.3. We used a spherical shell model with power law distributions for grain density and temperatures:

$$n(r)=n_o\,(r/R_o)^{-2} \qquad \text{and} \qquad T(r) = T_o\,(r/R_o)^{-.4}$$

as suggested by the rigorous models (Rowan-Robinson and Harris, 1982). For the present purposes, the more important parameters are :

- The colour temperature of the central star: T_*,
- The inner temperature of the shell : T_o,
- The optical thickness at 10 μm: τ_{10},
- The optical efficiency profile of dust: $Q(\lambda)$.

Equilibrium condensation computations of a gas of cosmic composition (Grossman, 1972) show that the first materials to condense will be SiO_4Mg_2 , then SiO_3Mg. We used their optical properties as measured by Day (1979) as zero-order

https://doi.org/10.1017/S0252921100084761 Published online by Cambridge University Press

approximation to those we want to deduce from the observations.

For each object, we first determine the parameters T_*, T_0 and τ_{10}, using the optical properties of SiO_3Mg or SiO_4Mg_2 and minimizing the quantity:

$$S^2 = \sum_\lambda \left\{ \left[F(\text{data}) - F(\text{model}) \right] / F(\text{data}) \right\}^2$$

We then modify the Q $(\lambda)/$ a values by an iterative process until we obtain a common profile for all the emission features and a common profile for all the absorption ones, which permit to best fit the individual spectra.

3. COMPARISON OF THE TWO PROFILES

Figures 3 and 4 show the comparison between data and model for the twelve objects in emission, and the thirteen in absorption. In every case, the residual discrepancy S is smaller than 15%. The resultant optical efficiency profiles are shown fig.5.

The a and b profiles are clearly distinguished by the wavelength of their maximum emissivity peak and by the depth of the 14 μm trough. Their principal properties are summarized in the table 1 below.
The average properties deduced from absorption spectra (b) are identical to those of amorphous enstatite: SiO_3Mg (residual discrepancy $< 9\%$), whereas those deduced from emission features (a) are close to those of amorphous forsterite: SiO_4Mg_2 (c), except between 12 and 16 μm where they are considerably stronger. Note that these differences must have a physical meaning since they are larger than the dispersion of individual profiles about their average (the length of one vertical bar is 2σ of the mean).

	CS shells (emission)	ISM (absorption)
principal component	SiO_4Mg_2	SiO_3Mg
λmax (μm)	10	9.5
HHFW (μm)	2.5	2
Q(10 μm)/Q(14 μm)	6	20

Table 1: Characteristics of observational Q $(\lambda)/$ Ao profiles.

4. DISCUSSION

Grossman (1972) shows that, in a cooling atmosphere, solid SiO_4Mg_2 condenses before solid SiO_3Mg then reacts with the gas to transform into the latter if enough time and solid-gas interface is available. The difference between the two profiles we deduced above is understood in the light of this result:

CIRCUMSTELLAR SHELLS:
Rather short residence time (10^3 years) .... } SiO_4Mg_2
Large radii (i.e. small area/volume for soldi-gas interaction) } SiO_4Mg_2
Relative movement of dust w.r.t. gas .... } SiO_4Mg_2

https://doi.org/10.1017/S0252921100084761 Published online by Cambridge University Press

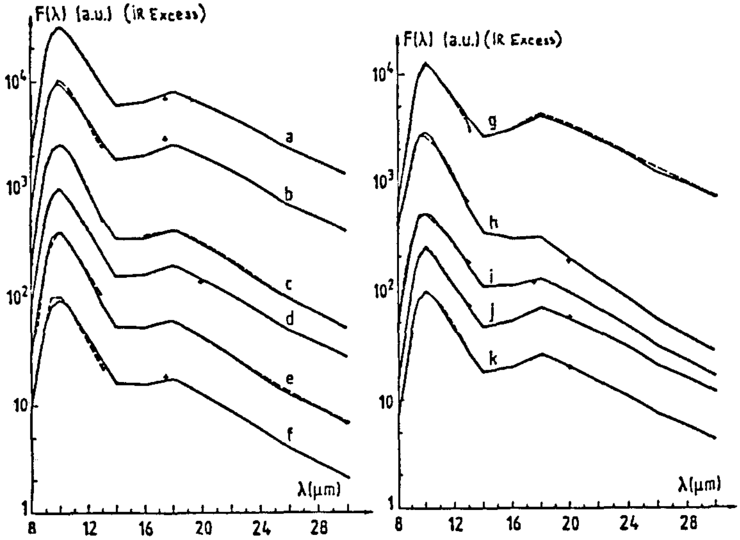

Fig.3 : Model (full line) and data (dashed line) for: a: V 915 Sco, b: HR 5171 A, c: μ Cep (1,2), d: RW Cyg (1), e: α Ori (1,2), f: K W Sgr, g: PZCas (2), h: VXSgr (1), i: UYSct, j: RSCnc (1), k: SLep. Data are from: (1) Merrill et al (1976) and (2) Forrest et al. (1979).

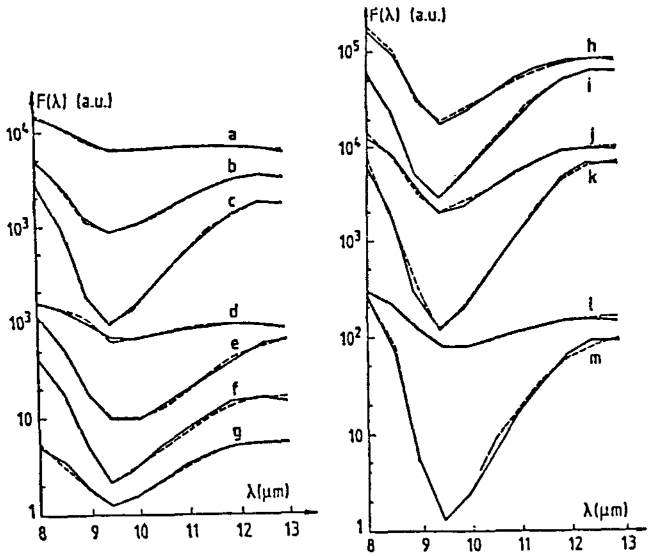

Fig.4: Same as fig.3 for absorption features: a: AFGL989, b: AFGL 2591, c: NGC 7538/IRS 1, d: AFGL 2059, e: S255/IRS1, f: AFGL 2136, g: AFGL 2884, h: NGC 7538/IRS 9, i: G 45.07 + 0.13, j: NGC 2170/IRS 3, k: W3/IRS5, l: BN, m: W 33. Data are from Willner et al (1982). Curves are arbitrarily displaced in the vertical direction for convenient display.

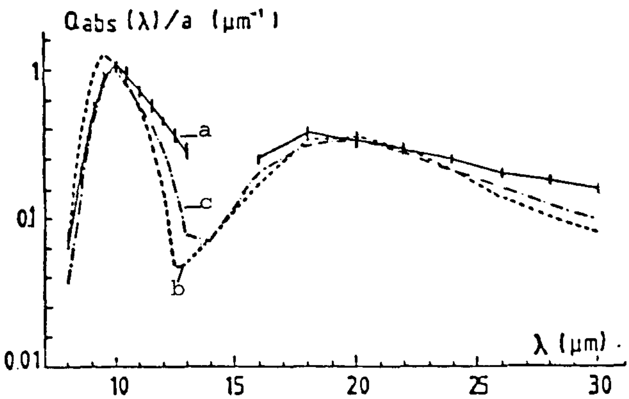

Fig.5 : Resultant Q (λ)/a profiles:
(a) : emission features,
(b) : absorption features Identical to pure SiO_3Mg_1
(c) : pure SiO_4Mg_2.

https://doi.org/10.1017/S0252921100084761 Published online by Cambridge University Press

GENERAL ISM:
Long residence time ------------------------------------ } SiO_3Mg
Small grains (i.e. large area/volume for solid-gas interaction)---- } SiO_3Mg

INTERMEDIATE CASE:
It is interesting to note that several cold oxygen-rich stars, with thick CS shells, display a narrow and shallow dip at ≈ 9.5 um super-imposed upon a wide emission feature of the SiO_4Mg_2 type. This could be interpreted as an equilibration of gas and dust at the envelope periphery resulting in the transformation of SiO_4Mg_2 into SiO_3Mg.

Herndon and Suess (1977) show that, in the condensate of a gas of solar composition, the larger the proportion of SiO_4Mg_2 is w.r.t. SiO_3Mg, the larger is the proportion of iron in the silicate phase. Our findings agree with this result because:
- The optical efficiency profile from emission spectra is consistent with a mixture of SiO_4Mg_2 and SiO_4Fe_2 taking into account the respective abundances of iron and magnesium.
While the optical efficiency profile from absorption spectra excludes other materials exhibiting strong spectral features between 8 and 30 µm, it permits the presence of metallic iron or FeS or any other material having a monotonous optical efficiency profile in this range of wavelength.

REFERENCES

Day, K.L., 1979, Astrophys. J., 234, 158.
Forrest, W.J., Mc Carthy, J.F., Houck, J.R., 1979, Astrophys. J., 233, 611.
Forrest, W.J., Gillett, F.C., Houck, J.R., Mc Carthy, J.F., Merrill, K.M., Pipher, J.L., Puetter, R.C., Russell, R.W., Soifer, B.T., Willner, S.P., 1978, Astrophys. J. , 219, 114.
Grossman, L., 1972, Geochim. Cosmochim. Acta, 36, 597.
Herndon, J.M., Suess, H.E., 1977, Geochim. Cosmochim. Acta, 41, 233.
Mc Carthy, J.F., Forrest, W.J., Briotta, D.A., Houck, J.R., 1980, Astrophys. J., 242, 965.
Merrill, K.M., Stein, W., 1976, Publ. Astron. Soc. Pacific, 88, 285.
Papoular, R., Pegourie, B., 1983, Astron. Astrophys., 128, 335.
Rowan-Robinson, M., Harris, S., 1982, Monthly Notices Roy. Astron.Soc., 200, 197.
Seki, J., Hasegawa, H., 1981, Progr. Theo. Phys., 66, 903.
Willner, S.P., Gillett, F.C., Herter, T.L., Jones, B., Krassner, J., Merrill, K.M., Pipher, J.L., Puetter, R.C., Rudy,R.J., Russell, R.W., Soifer, B.T., 1982, Astrophys. J., 253, 174.
Woolf, N.J., Ney, E.P., 1969, Astrophys. J., 155, L181.
Woolf, N.J., 1973, in "Interstellar Dust and Related Topics", IAU Symposium n° 52, ed. J.M. Greenberg and H.C. Van de Hulst, (Reidel), 485.

https://doi.org/10.1017/S0252921100084761 Published online by Cambridge University Press